 DOR: 20.1001.1.2322388.2021.9.1.4.0

Research Paper

Influence of Power Law Distribution with Pressure on the Frequencies of Supported Functionally Graded Material Cylindrical Shell with C-SL and F-SS Boundary Conditions

Mohammadreza Isvandzibaei*

Department of Mechanical Engineering, Andimeshk Branch, Islamic Azad University, Andimeshk, Iran

ARTICLE INFO

Article history:

Received 24 July 2020
Accepted 6 August 2020
Available online 1 January 2021

Keywords:

*Power law distribution
Frequency
Pressure
Cylindrical Shell
FGM*

ABSTRACT

In this paper, influence power-law distribution with pressure on frequencies of the supported functionally graded cylindrical shell is studied. This shell is constructed from a functionally graded material (FGM) with two constituent materials. FGMs are graded through the thickness direction, from one surface of the shell to the next. The supported FGM shell equations are created based on FSDT. The governing equations of the movement were utilized by the Ritz method. The boundary conditions are clamp-sliding and free-simply support. The influence of the various values of the power-law distribution with pressure supported and different conditions on the frequencies characteristics are studied. This study shows that the frequencies decreased with the increase in the amounts of the power-law distribution with pressure. Thus, the constituent power-law distribution with pressure effects on the frequencies. The results show the frequencies with different power-law distribution under pressures are various for different conditions.

* **Corresponding author:**

E-mail address: esvandzebaei@yahoo.com

1. Introduction

In all of the world, applications of cylindrical shells have developed in science. Cylindrical shells have extensive applications in engineering and industry. The study of the vibratory response of cylindrical shells is very significant for the behavior and applications of these structures. Some of these applications are found in the aerospace, civil, mechanical, and maritime construction development [1].

Some researchers for eschew failure are used stiffener shells [2-7]. Vibration cylindrical shells are an important subject of research by scientists, and it was first presented via love [8]. Natural frequencies, several theories, and boundary conditions were introduced via Leissa [9], Blevins [10], Soedel [11], Chung [12], Reddy [13], and Forsberg [14].

Functionally graded materials (FGMs) are constructed by mixing various materials, and they are graded in thickness. These materials comprise a blend of metal and ceramic or other different materials. Also, the physical properties of one level vary from the other level, and these materials are generated by the composition of two or more materials.

For the sample, one level has thermo resistant, and the other level has mechanical properties. The main benefit of FGMs is their application in environments with high temperatures. FGM structures are utilized as coatings space schemes, spacecraft, reactors, turbines, components in engines, and others [15]. Research on the shells made of FGM is significant in the engineering applications.

The significant research on FGM shell was reported by Loy [16]. The finite element method on FGM cylindrical shells was used by Patel et al. [17]. Study frequencies with effects of radius published by Zhi and Hu [18]. Arshad et al. [19] and Shah et al. [20] investigated the frequency characteristic of FGM cylindrical shells. Hosseini et al. [21] investigated rotating functionally graded cylindrical shell. Amirabadi et al. [22] studied vibration FGM GPL-reinforced truncated thick conical shells under different boundary conditions. They showed that dispersing more GPL reinforcements near the inner and outer surfaces of the rotating shells leads to a remarkable increase in both forward and backward wave frequencies. Mohammadi et al. [23] investigated numerical investigation of nonlinear vibration analysis for triple-walled carbon nanotubes conveying viscous fluid. Amirabadi et al. [24] studied wave propagation in rotating functionally graded GPL-reinforced cylindrical shells based on the third-order shear deformation theory.

The object of this study is to the analysis influence of power-law distribution with pressure on frequencies of the supported functionally graded cylindrical shell. The

analysis is done based on the first-order theory. The governing equations of the movement were utilized by Ritz method. The boundary conditions are clamp-sliding (C-SL) and free-simply support (F-SS).

The influence of the various values of the power-law distribution with pressure supported and different conditions on the frequencies characteristics are discussed. The accuracy of this procedure is confirmed by comparisons the present results with other ones that existed in literature.

2. Functionally Graded Materials

FGMs are made of the variation of composition and different materials. The volume fraction distribution of each phase of material varies with a specific gradient. The E_{fgm} , ν_{fgm} and ρ_{fgm} are given as:

$$E_{fgm}(T, z) = (E_2(T) - E_1(T)) \left(z + \frac{h}{2} / h \right)^N + E_1(T) \quad (1)$$

$$\nu_{fgm}(T, z) = (\nu_2(T) - \nu_1(T)) \left(z + \frac{h}{2} / h \right)^N + \nu_1(T) \quad (2)$$

$$\rho_{fgm}(T, z) = (\rho_2(T) - \rho_1(T)) \left(z + \frac{h}{2} / h \right)^N + \rho_1(T) \quad (3)$$

3. First order Shear Deformation Theory

Consider figure 1, in which a geometrical sketch of reinforced FGM cylindrical shell under pressure is given. The displacement field with first-order theory is written as

$$\begin{aligned} u(x, \theta, z) &= u_0(x, \theta) + z\psi_x(x, \theta) \\ v(x, \theta, z) &= v_0(x, \theta) + z\psi_\theta(x, \theta) \end{aligned} \quad (4)$$

$$w(x, \theta, z) = w_0(x, \theta)$$

The strain displacement relationships are expressed by

$$\varepsilon_{11} = \frac{1}{A_1} \frac{\partial u(x, \theta, z)}{\partial x} + \frac{1}{A_1 A_2} \frac{\partial A_1}{\partial \theta} v(x, \theta, z) + \frac{w(x, \theta, z)}{R_1} \quad (5)$$

$$\varepsilon_{22} = \frac{1}{A_2} \frac{\partial v(x, \theta, z)}{\partial \theta} + \frac{1}{A_1 A_2} \frac{\partial A_2}{\partial x} u(x, \theta, z) + \frac{w(x, \theta, z)}{R_2} \quad (6)$$

$$\varepsilon_{12} = \frac{A_2}{A_1} \frac{\partial}{\partial x} \left(\frac{v(x, \theta, z)}{A_2} \right) + \frac{A_1}{A_2} \frac{\partial}{\partial \theta} \left(\frac{u(x, \theta, z)}{A_1} \right) \quad (7)$$

$$\varepsilon_{13} = A_1 \frac{\partial}{\partial z} \left(\frac{u(x, \theta, z)}{A_1} \right) + \frac{1}{A_1} \frac{\partial w(x, \theta, z)}{\partial x} \quad (8)$$

$$\varepsilon_{23} = A_2 \frac{\partial}{\partial z} \left(\frac{v(x, \theta, z)}{A_2} \right) + \frac{1}{A_2} \frac{\partial w(x, \theta, z)}{\partial \theta} \quad (9)$$

$$\varepsilon_{33} = 0 \quad (10)$$

where A_1 and A_2 are the parameters of Lamé [25].

$$A_1 = \frac{\partial r}{\partial x} \quad A_2 = \frac{\partial r}{\partial \theta} \quad (11)$$

Substituting Eq. (4) into Eqs. (5-9), thus

$$\bar{\varepsilon}_{11} = \frac{\partial u_0(x, \theta)}{\partial x} + z \frac{\partial \psi_x(x, \theta)}{\partial x} \quad (12)$$

$$\bar{\varepsilon}_{22} = \frac{\partial v_0(x, \theta)}{R \partial \theta} + z \frac{\partial \psi_\theta(x, \theta)}{R \partial \theta} + \frac{w_0(x, \theta)}{R} \quad (13)$$

$$\bar{\varepsilon}_{12} = \frac{\partial v_0(x, \theta)}{\partial x} + \frac{\partial u_0(x, \theta)}{R \partial \theta} + z \left(\frac{\partial \psi_x(x, \theta)}{R \partial \theta} + \frac{\partial \psi_\theta(x, \theta)}{\partial x} \right) \quad (14)$$

$$\bar{\varepsilon}_{13} = \psi_x(x, \theta) + \frac{\partial w_0(x, \theta)}{\partial x} \quad (15)$$

$$\bar{\varepsilon}_{23} = \psi_\theta(x, \theta) + \frac{\partial w_0(x, \theta)}{R \partial \theta} \quad (16)$$

The stress-strain equations are written by

$$\{\bar{\sigma}\} = [\bar{Q}] \{\bar{\varepsilon}\} \quad (17)$$

where

$$\{\bar{\sigma}\}^T = \{\bar{\sigma}_{11} \quad \bar{\sigma}_{22} \quad \bar{\sigma}_{12} \quad \bar{\sigma}_{13} \quad \bar{\sigma}_{23}\} \quad (18)$$

$$\{\bar{\varepsilon}\}^T = \{\bar{\varepsilon}_{11} \quad \bar{\varepsilon}_{22} \quad \bar{\varepsilon}_{12} \quad \bar{\varepsilon}_{13} \quad \bar{\varepsilon}_{23}\} \quad (19)$$

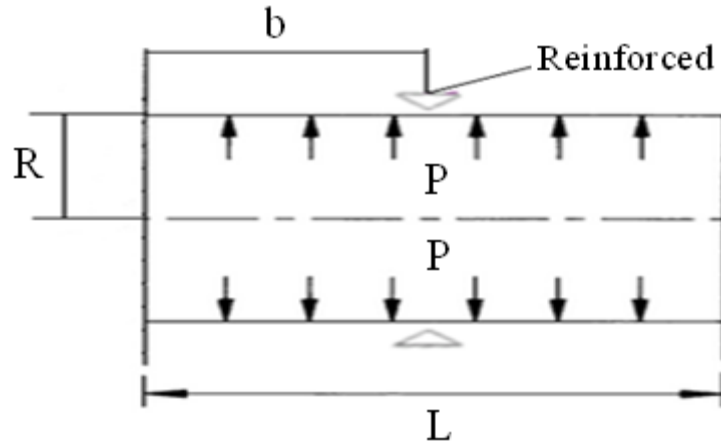


Fig. 1. The supported FGM cylindrical shell with pressure

$$[\bar{Q}] = \begin{bmatrix} \bar{Q}_{11} & \bar{Q}_{12} & 0 & 0 & 0 \\ \bar{Q}_{21} & \bar{Q}_{22} & 0 & 0 & 0 \\ 0 & 0 & \bar{Q}_{66} & 0 & 0 \\ 0 & 0 & 0 & \bar{Q}_{55} & 0 \\ 0 & 0 & 0 & 0 & \bar{Q}_{44} \end{bmatrix} \quad (20)$$

$$\bar{Q}_{55} = K \frac{E(z)}{2(1-\nu(z))} \quad A = 1 + \frac{z}{R} \quad (25)$$

where $K = 5/6$ [26].

The moment resultants are:

$$\{N_x, N_\theta, N_{x\theta}, H_x, H_\theta\} = \int_{-h/2}^{h/2} \{\bar{\sigma}_{11} \quad \bar{\sigma}_{22} \quad \bar{\sigma}_{12} \quad \bar{\sigma}_{13} \quad \bar{\sigma}_{23}\} dz \quad (26)$$

$$\{M_x, M_\theta, M_{x\theta}\} = \int_{-h/2}^{h/2} \{\bar{\sigma}_{11} \quad \bar{\sigma}_{22} \quad \bar{\sigma}_{12}\} z dz \quad (27)$$

Applying Eqs.(12-16) into Eq.(21) and substituting in Eqs.(26) and (27) the following equation is got

$$\{N\} = [I] \{\bar{\varepsilon}\} \quad (28)$$

where $\{N\}$, $\{\bar{\varepsilon}\}$ and $[I]$ are

$$\{N\}^T = \{N_x, N_\theta, N_{x\theta}, M_x, M_\theta, M_{x\theta}, H_x, H_\theta\} \quad (29)$$

$$\{\bar{\varepsilon}\}^T = \{\bar{\varepsilon}_{11} \quad \bar{\varepsilon}_{22} \quad \bar{\varepsilon}_{12} \quad \bar{\varepsilon}_{13} \quad \bar{\varepsilon}_{23}\} \quad (30)$$

Then equation (17) can be expressed as

$$\begin{Bmatrix} \bar{\sigma}_{11} \\ \bar{\sigma}_{22} \\ \bar{\sigma}_{12} \\ \bar{\sigma}_{13} \\ \bar{\sigma}_{23} \end{Bmatrix} = \begin{bmatrix} \bar{Q}_{11} & \bar{Q}_{12} & 0 & 0 & 0 \\ \bar{Q}_{21} & \bar{Q}_{22} & 0 & 0 & 0 \\ 0 & 0 & \bar{Q}_{66} & 0 & 0 \\ 0 & 0 & 0 & \bar{Q}_{55} & 0 \\ 0 & 0 & 0 & 0 & \bar{Q}_{44} \end{bmatrix} \begin{Bmatrix} \bar{\varepsilon}_{11} \\ \bar{\varepsilon}_{22} \\ \bar{\varepsilon}_{12} \\ \bar{\varepsilon}_{13} \\ \bar{\varepsilon}_{23} \end{Bmatrix} \quad (21)$$

The stiffness is written as

$$\bar{Q}_{11} = \frac{E(z)}{1-\nu^2(z)}, \bar{Q}_{12} = \frac{\nu(z)E(z)}{A(1-\nu^2(z))} \quad (22)$$

$$\bar{Q}_{21} = \frac{\nu(z)E(z)}{1-\nu^2(z)}, \bar{Q}_{22} = \frac{E(z)}{A(1-\nu^2(z))} \quad (23)$$

$$\bar{Q}_{66} = \frac{E(z)}{2A(1-\nu(z))}, \bar{Q}_{44} = K \frac{E(z)}{2(1-\nu(z))} \quad (24)$$

$$[I] = \begin{bmatrix} X_{11} & X_{12} & X_{16} & Y_{11} & Y_{12} & Y_{16} & 0 & 0 \\ X_{12} & X_{22} & X_{26} & Y_{12} & Y_{22} & Y_{26} & 0 & 0 \\ X_{16} & X_{26} & X_{66} & Y_{16} & Y_{26} & Y_{66} & 0 & 0 \\ Y_{11} & Y_{12} & Y_{16} & Z_{11} & Z_{12} & Z_{16} & 0 & 0 \\ Y_{12} & Y_{22} & Y_{26} & Z_{12} & Z_{22} & Z_{26} & 0 & 0 \\ Y_{16} & Y_{26} & Y_{66} & Z_{16} & Z_{26} & Z_{66} & 0 & 0 \\ 0 & 0 & 0 & 0 & 0 & 0 & kV_{44} & kV_{45} \\ 0 & 0 & 0 & 0 & 0 & 0 & kV_{45} & kV_{55} \end{bmatrix} \quad (31)$$

in which X_{ij}, Y_{ij}, Z_{ij} and V_{ij} are

$$(X_{ij}, Y_{ij}, Z_{ij}) = \int_{-h/2}^{h/2} Q_{ij}(1, Z, Z^2) dz \quad V_{ij} = K \int_{-h/2}^{h/2} Q_{ij} dz \quad (32)$$

4 Energy Equations

The strain energy is expressed as

$$U = \frac{1}{2} \int_0^L \int_0^{2\pi} \left\{ \begin{matrix} \varepsilon \\ \varepsilon \end{matrix} \right\}^T [II] \left\{ \begin{matrix} \varepsilon \\ \varepsilon \end{matrix} \right\} R d\theta dx \quad (33)$$

The kinetic energy is given by

$$T = \frac{1}{2} \int_0^L \int_0^{2\pi} \rho T \left\{ \left(\frac{\partial u_0(x, \theta)}{\partial t} \right)^2 + \left(\frac{\partial v_0(x, \theta)}{\partial t} \right)^2 + \left(\frac{\partial w_0(x, \theta)}{\partial t} \right)^2 + \left(\frac{\partial \psi_x(x, \theta)}{\partial t} \right)^2 + \left(\frac{\partial \psi_\theta(x, \theta)}{\partial t} \right)^2 \right\} R d\theta dx \quad (34)$$

The potential energy of pressure is

$$V = \int_0^L \int_0^{2\pi} \frac{P}{2} \left\{ \frac{\partial^2 w_0(x, \theta)}{\partial \theta^2} + w_0(x, \theta) \right\} w_0(x, \theta) d\theta dx \quad (35)$$

Therefore, the energy functional can be written as

$$F = U - T + V \quad (36)$$

5 Boundary Conditions

The displacement field can be expressed as

$$\begin{aligned} u_0(x, \theta) &= \bar{E}_1 \frac{\partial \Omega(x)}{\partial x} \cos(n\theta) \cos(\omega t) \\ v_0(x, \theta) &= \bar{E}_2 \Omega(x) \sin(n\theta) \cos(\omega t) \\ w_0(x, \theta) &= \bar{E}_3 \Omega(x) \prod_{i=1}^H (x - b_i)^{\mu_i} \cos(n\theta) \cos(\omega t) \\ \psi_x(x, \theta) &= \bar{E}_4 \frac{\partial \Omega(x)}{\partial x} \cos(n\theta) \cos(\omega t) \\ \psi_\theta(x, \theta) &= \bar{E}_5 \Omega(x) \sin(n\theta) \cos(\omega t) \end{aligned} \quad (37)$$

where $\Omega(x)$ is beam function can be expressed as

$$\begin{aligned} \Omega(x) &= \Psi_1 \cosh\left(\frac{\Phi_m x}{L}\right) + \Psi_2 \cos\left(\frac{\Phi_m x}{L}\right) - \mu_m (\Psi_3 \sinh\left(\frac{\Phi_m x}{L}\right) \\ &+ \Psi_4 \sin\left(\frac{\Phi_m x}{L}\right)) \end{aligned} \quad (38)$$

6 Ritz Method

The energy functional, F expressed with Lagrangian function

$$F = U_{\max} - T_{\max} + V_{\max} \quad (39)$$

Substituting Eq. (37) in Eqs. (33), (34) and (35) and minimizing:

$$\left. \begin{aligned} \frac{\partial (U_{\max} - T_{\max} + V_{\max})}{\partial \bar{E}_1} &= 0 \\ \frac{\partial (U_{\max} - T_{\max} + V_{\max})}{\partial \bar{E}_2} &= 0 \\ \frac{\partial (U_{\max} - T_{\max} + V_{\max})}{\partial \bar{E}_3} &= 0 \\ \frac{\partial (U_{\max} - T_{\max} + V_{\max})}{\partial \bar{E}_4} &= 0 \\ \frac{\partial (U_{\max} - T_{\max} + V_{\max})}{\partial \bar{E}_5} &= 0 \end{aligned} \right\} \quad (40)$$

The governing equation with matrix form is

$$\begin{bmatrix} C_{11} & C_{12} & C_{13} & C_{14} & C_{15} \\ C_{21} & C_{22} & C_{23} & C_{24} & C_{25} \\ C_{31} & C_{32} & C_{33} & C_{34} & C_{35} \\ C_{41} & C_{42} & C_{43} & C_{44} & C_{45} \\ C_{51} & C_{52} & C_{53} & C_{54} & C_{55} \end{bmatrix} \begin{Bmatrix} \bar{E}_1 \\ \bar{E}_2 \\ \bar{E}_3 \\ \bar{E}_4 \\ \bar{E}_5 \end{Bmatrix} = \begin{Bmatrix} 0 \\ 0 \\ 0 \\ 0 \\ 0 \end{Bmatrix} \quad (41)$$

The determinant of matrix C equals to zero

$$|C_{ij}| = 0 \quad (42)$$

with solution equation (42):

$$\delta_0 \omega^{10} + \delta_1 \omega^8 + \delta_2 \omega^6 + \delta_3 \omega^4 + \delta_4 \omega^2 + \delta_5 = 0 \quad (43)$$

The equation (43) is consists of ten roots, and the smallest positive root is the natural frequency in the present research. The properties of materials are specified in Table 2.

Table 1 Values of Ψ_i, Φ_m and μ_m for asymmetric boundary conditions [5].

BC	$\Psi_i (i=1, \dots, 4)$	Φ_m	μ_m
C-SL	$\Psi_1 = 1, \Psi_2 = -1$ $\Psi_3 = 1, \Psi_4 = -1$	$(4m - 1)\pi / 4$	$\frac{\cosh \Phi_m - \cos \Phi_m}{\sinh \Phi_m - \sin \Phi_m}$
F-SS	$\Psi_1 = 1, \Psi_2 = 1$ $\Psi_3 = 1, \Psi_4 = 1$	$(4m + 1)\pi / 4$	$\frac{\cosh \Phi_m - \cos \Phi_m}{\sinh \Phi_m - \sin \Phi_m}$

Table 2 Mechanical properties of materials [16].

Coefficients of temperature	Stainless Steel			Nickel		
	$E(Nm^{-2})$	ν	$\rho(kgm^{-3})$	$E(Nm^{-2})$	ν	$\rho(kgm^{-3})$
Q^0	201.04×10^9	0.3262	8166	223.95×10^9	0.3100	8900
Q^{-1}	0	0	0	0	0	0
Q^1	3.079×10^{-4}	-2.002×10^{-4}	0	-2.794×10^{-4}	0	0
Q^2	-6.534×10^{-7}	3.797×10^{-7}	0	-3.998×10^{-9}	0	0
Q^3	0	0	0	0	0	0
Q	2.07788×10^{11}	0.317756	8166	2.05098×10^{11}	0.3100	8900

Table 3 Natural frequency of FGM cylindrical shell without support and pressure ($R = 1, N = 1, L/R = 20$).

h/R	m	n	Natural frequency (Hz)	
			Loy et al. [16]	Present
0.002	1	1	13.211	13.186
	1	2	4.480	4.4200
	1	3	4.1569	4.0346
	1	4	7.0384	7.0240
	1	5	11.241	11.124
	1	6	16.455	16.221
	1	7	22.635	22.306
	1	8	29.771	30.111
	1	9	37.862	37.560
	1	10	46.905	46.397

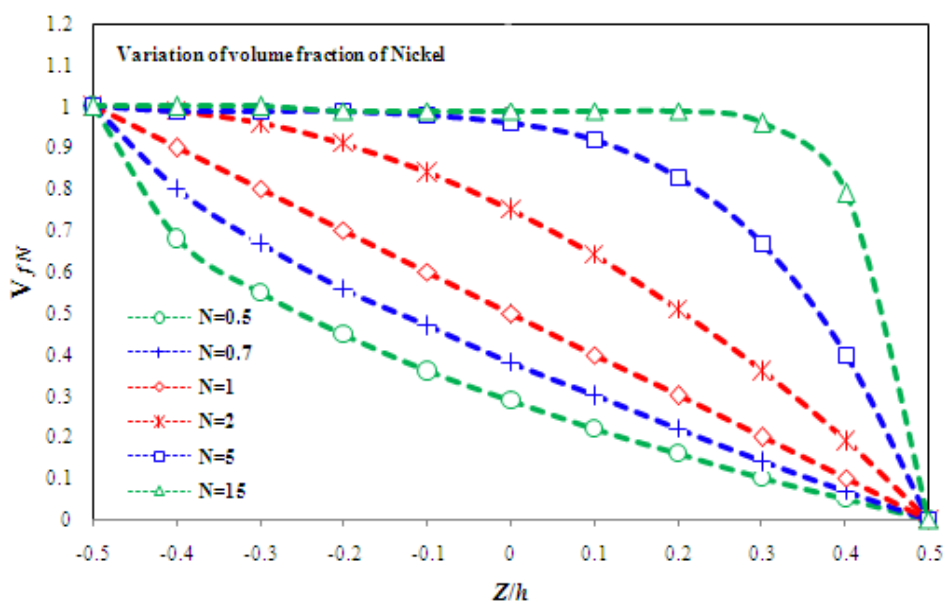


Fig. 2. Volume fraction of Nickel V_{fN} with thickness variable Z/h

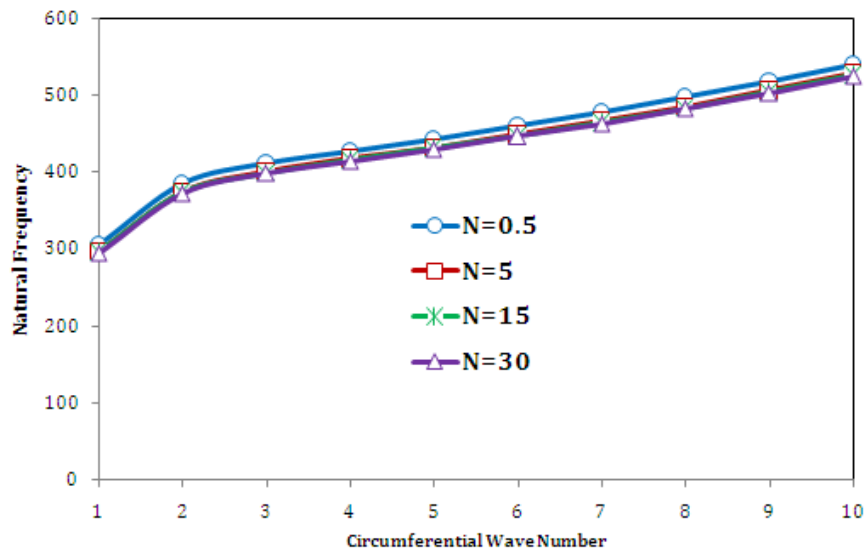


Fig. 3. Changes of frequency with support and pressure for different power law under C-SL (P = 700 KPa, h/R = 0.002, L/R = 20, b= 0.5L)

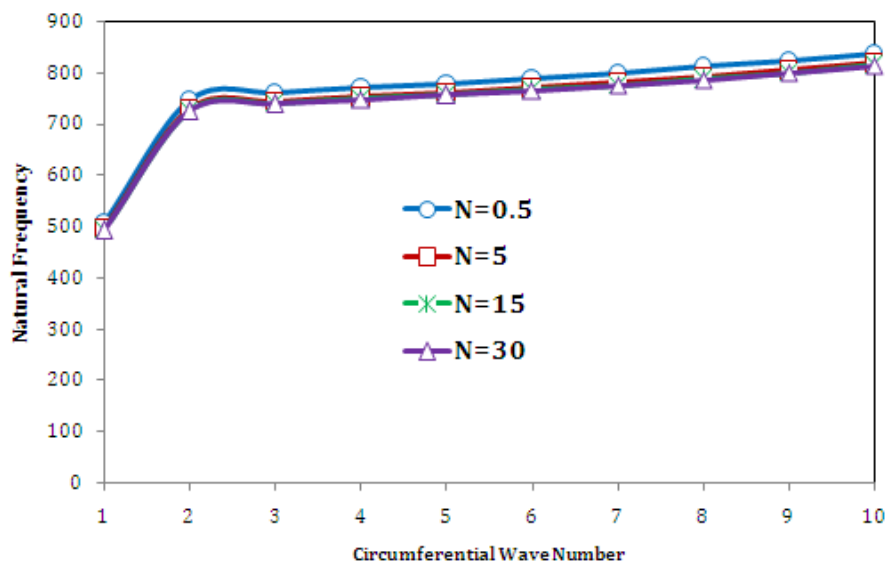


Fig. 4. Changes of frequency with support and pressure for different power law under F-SS (P = 700 KPa, h/R = 0.002, L/R = 20, b= 0.5L)

7 Comparison Study

To validate of the present study, the results of the FGM cylindrical shell without pressure and support are evaluated with the results in other literature. Table 3 shows the variation of the frequency for the FGM cylindrical shell without pressure and support with two different h/R ratios. The comparisons presented in Table 3, show good agreeable results with published works.

8 Results and Discussion

Variation of volume fractions of Nickel is shown in Fig. 2. In this figure the volume fraction of nickel V_{fN} decreased from value 1 at $z/h = -0.5$ to its least value 0 at $z/h = +0.5$. For $z/h < 0$ and $N < 1$, the decrease of V_{fN} is rapid. For $z/h < 0$ and $N > 1$, the rate of

decrease of V_{fN} is slow while for $z/h > 0$ and $N > 1$, it decreases rapidly. It is observed that the variations of the constituent material for FGMs are influenced by the volume fraction laws.

Tables 4 and 5 show variations of the frequency with different power-law distribution with pressure. The frequencies are discussed for different (N). In these tables, different values of power-law with pressures efficacy frequency of supported FGM cylindrical shell. In these tables, $m=1$ and it is mean first axial wave mode used in this analysis. For $m>1$ simulation result was found to yield similar trends for two asymmetric boundary conditions. The decrease in the frequencies from $N = 0.5$ to $N = 30$ is about 3.156% at $n = 1$ and 3.095% at $n = 10$. Therefore, the arrangement of constituent materials in FGMs will determine the

increment and decrements in the natural frequency with power-law distribution. The results show the natural frequencies for various power-law with pressure are various for boundary conditions.

Figures 3 and 4 depict a variation of frequency with support and pressure for a different power-law distribution. In both cases C–SL and F–SS, the frequencies for the different power-law with pressure increase with the circumferential wave number.

In these figures, when reinforcement is used, significant changes in the natural frequency are

observed at low circumferential wave numbers. It can be seen from these figures that the increase in natural frequency is significant when n increased from 1 to 2, and for n greater than 2, the natural frequency increases gradually as the circumferential wave number n is increased. The results show that power-law distribution has an effect on the natural frequency, and frequencies decreased with the increase in the power-law distribution.

Table 4 Variation of the natural frequency (Hz) with the different power-law exponent for C-SL boundary conditions ($h/R = 0.002, L/R = 20$)

n	m	$P = 700 \text{ kPa}, a/L = 0.5$			
		$N = 0.5$	$N = 5$	$N = 15$	$N = 30$
1	1	342.546	334.567	332.903	331.509
2	1	429.875	419.132	417.519	416.220
3	1	456.345	445.094	442.763	442.729
4	1	473.980	461.342	458.093	458.228
5	1	487.124	475.228	473.773	472.541
6	1	502.569	490.632	488.387	487.118
7	1	519.320	506.096	504.531	503.539
8	1	537.671	524.667	521.335	521.447
9	1	556.905	543.491	541.822	540.731
10	1	577.428	564.611	561.747	561.983

Table 5 Variation of the natural frequency (Hz) with the different power-law exponent for F-SS boundary conditions ($h/R = 0.002, L/R = 20$)

n	m	$P = 700 \text{ kPa}, a/L = 0.5$			
		$N = 0.5$	$N = 5$	$N = 15$	$N = 30$
1	1	480.679	469.240	466.942	466.670
2	1	800.226	780.754	777.405	775.051
3	1	810.076	791.744	787.116	785.565
4	1	817.676	797.311	793.242	792.111
5	1	826.913	806.962	800.899	800.533
6	1	833.346	812.670	808.920	807.872
7	1	842.118	822.749	818.442	817.276
8	1	853.842	833.286	829.091	827.878
9	1	866.894	845.462	841.295	838.369
10	1	879.643	858.961	854.581	853.665

9 Conclusions

This study presents the influence of power-law distribution with pressure on frequencies of the supported functionally graded cylindrical shell. The governing equations of the movement were utilized by the Ritz method. The boundary conditions are clamp-

sliding and free- simply support. Natural frequencies with different amounts of the power-law with pressure for different boundary conditions are affected by the variation of the circumferential wave number. This study shows that the frequencies decreased with the increase in the amounts of the power-law distribution

with pressure. Thus the constituent power-law distribution with pressure effects on the frequencies. The results show the frequencies with different power-law distribution under pressures are various for different conditions.

References

- [1] Sechler, E.E., 1974. Thin-shell structures theory experiment and design. Englewood Cliffs, NJ: Prentice-Hall, California.
- [2] Yan, J., Li, T.Y., Liu, T.G. & Liu, J.X. 2006. Characteristics of the vibrational power flow propagation in a submerged periodic ring-stiffened cylindrical shell. *Applied Acoustics*. (67): 550-569.
- [3] Wang, R.T. & Lin, Z.X. 2006. Vibration analysis of ring-stiffened cross-ply laminated cylindrical shells. *Journal of Sound and Vibration*. (295): 964-987.
- [4] Pan, Z., Li, X. & Ma, J. A. 2008. Study on free vibration of a ring-stiffened thin circular cylindrical shell with arbitrary boundary conditions. *Journal of Sound and Vibration*. (314): 330-342.
- [5] Gan, L., Li, X. & Zhang, Z. 2009. Free vibration analysis of ring-stiffened cylindrical shells using wave propagation approach. *Journal of Sound and Vibration*. (326): 633-646.
- [6] Zhou, X. 2012. Vibration and stability of ring-stiffened thin-walled cylindrical shells conveying fluid. *Acta Mechanica Sinica*. (25): 168-176.
- [7] Qu, Y., Chen, Y., Long, X., Hua, H. & Meng, G. 2013. A modified variational approach for vibration analysis of ring-stiffened conical-cylindrical shell combinations. *European Journal of Mechanics endash; A/Solids*. (37): 200-215.
- [8] Love, A.E.H. 1944. A treatise on the mathematical theory of elasticity [M]. New York: Dover Publication.
- [9] Leissa, A.W. 1993. Vibration of shells. NASA SP-288, 1973; Reprinted by Acoustical Society of America, America Institute of Physics.
- [10] Blevins, R.D. 1979. Formulas for natural frequency and mode shape. Van Nostrand Reinhold, New York.
- [11] Soedel, W. 1980. A new frequency formula for closed circular cylindrical shells for a large variety of boundary conditions. *Journal of Sound and Vibration*. (70): 309-317.
- [12] Chung, H. 1981. Free vibration analysis of circular cylindrical shells. *Journal of Sound and Vibration*. (74): 331-359.
- [13] Reddy, J.N. 2004. Mechanics of laminated composite plates and shells. 2nd edn. CRC Press, New York.
- [14] Forsberg, K. 1964. Influence of boundary conditions on modal characteristics of cylindrical shells. *AIAA Journal*. (2): 182-189.
- [15] Miyamoto, Y., Kaysser, W.A., Rabin, B.H., Kawasaki, A. & Ford, R.G. 1999. Functionally graded materials: design, processing and applications, Kluwer Academic Publishers, London.
- [16] Loy, C.T., Lam, K.Y. & Reddy, J.N. 1999. Vibration of functionally graded cylindrical shells. *International Journal of Mechanical Sciences*. (41): 309-324.
- [17] Patel, B.P., Gupta, S.S., Loknath, M.S. & Kadu, C.P. 2005. Free vibration analysis of functionally graded elliptical cylindrical shells using higher order theory. *Composite Structures*. (69): 259-270.
- [18] Zhi, C. & Hua, W. 2007. Free vibration of FGM cylindrical shells with holes under various boundary conditions. *Journal of Sound and Vibration*. (306): 227-237.
- [19] Arshad, S. H., Naeem, M. N., & Sultana, N. 2007. Frequency analysis of functionally graded material cylindrical shells with various volume fraction laws. *Proceedings of the Institution of Mechanical Engineers, Part C: Journal of Mechanical Engineering Science*. (221): 1483-1495.
- [20] Shah, A.G., Mahmood, T. & Naeem, M.N. 2009. Vibrations of FGM thin cylindrical shells with exponential volume fraction law. *Applied Mathematics and Mechanics (English Edition)*. (5): 607-615.
- [21] Hosseini-Hashemi, sh., Ilkhani, M.R and Fadaee, M. Accurate natural frequencies and critical speeds of a rotating functionally graded moderately thick cylindrical shell. *International Journal of Mechanical Sciences* 76 (2013) 9-20.
- [22] Amirabadi, H., Farhatnia, F., Eftekhari, S.A., Hosseini-Ara, R. 2020. Free vibration analysis of rotating functionally graded GPL-reinforced truncated thick conical shells under different boundary conditions. *Mechanics Based Design of Structures and Machines*, Published online: 30 Sep 2020. pp. 1-32.
- [23] Mohamadi, B., Eftekhari, S.A., Toghraie, D. 2020. Numerical investigation of nonlinear vibration analysis for triple-walled carbon nanotubes conveying viscous fluid. *International Journal of Numerical Methods for Heat & Fluid Flow*, Vol. 30 No. 4, pp. 1689-1723.
- [24] Amirabadi, H., Farhatnia, F., Eftekhari, S.A., Hosseini-Ara, R. 2021. Wave propagation in rotating functionally graded GPL-reinforced cylindrical shells based on the third-order shear deformation theory. *Waves in Random and Complex Media*, Published online: 03 Feb 2021.
- [25] Soedel, W. 2004. Vibration of shells and plates. 3rd edn. Marcel Dekker Inc, New York.
- [26] Reddy, J.N. 2004. Mechanics of laminated composite plates and shells: Theory and analysis, 2nd ed. CRC Press, Boca Raton.